

Electrochemical behavior and Li Diffusion study of LiCoO_2 thin film electrodes prepared by PLD

H. XIA^a, Y.S. MENG^b, L. LU^{a, c}, G. CEDER^{a, b}

^a Advanced Materials for Micro- and Nano- System, Singapore-MIT Alliance, 4 Engineering Drive 3, 117576 Singapore

^b Department of Materials Science and Engineering, Massachusetts Institute of Technology, Cambridge, MA 02139, USA

^c Department of Mechanical Engineering, National University of Singapore, 9 Engineering Drive 1, 117576 Singapore

Abstract — Preferred c-axis oriented LiCoO_2 thin films were prepared on the SiO_2/Si (SOS) substrates by pulsed laser deposition (PLD). Thin film electrodes without carbon and binder are ideal samples to study the electrochemical properties of materials. We did galvanostatic charge/discharge measurements between 3 and 4.7 V on the Li/LiCoO_2 cell to study its electrochemical behavior. Potentiostatic intermittent titration technique (PITT) was used to measure the Li diffusivity in the Li_xCoO_2 film at different Li concentrations ($0.15 < x < 0.75$). The dependence of Li diffusivity on the c-lattice parameter and valence of cobalt ions is discussed.

Keywords — LiCoO_2 ; Thin film; Li diffusion; Pulsed laser deposition

I. INTRODUCTION

FOR lithium-ion batteries, LiCoO_2 is the most commonly used cathode material due to its high capacity and good cyclability [1-2]. Though its theoretical capacity is 272 mAh/g, the reversible capacity is limited to 140 mAh/g when the LiCoO_2 is cycled between 3 and 4.2 V, corresponding to extracting and inserting about 0.5 Li per LiCoO_2 . In order to obtain higher capacity from LiCoO_2 , a cutoff voltage above 4.2 V must be applied which sometimes results in a rapid capacity loss. Because of the increasing interest in charging LiCoO_2 to voltage above 4.2 V, it is necessary to investigate the electrochemical behavior above 4.2 V.

Lithium diffusion in the electrodes is a key factor that determines the rate at which a battery can be charged and discharged. With increasing interest in high power density, the kinetics of Li diffusion becomes more important. Many diffusion measurements on LiCoO_2 have been performed on composite electrodes consisting of graphite, binders and other materials. However, a detailed analysis of diffusion coefficients is difficult for composite electrodes because of their non-uniform potential distributions and unknown

electrode surface area. Without carbon and binder, thin film electrodes are ideal samples to investigate the intrinsic properties of materials. The dense and flat thin film electrode with known composition and well-defined geometry may be more appropriate for diffusion measurements.

LiCoO_2 thin film electrodes have been successfully prepared by various techniques such as radio frequency (rf) sputtering [3], pulsed laser deposition (PLD) [4], chemical vapor deposition [5], spin coating [6] and electrostatic spray deposition (ESD) [7]. Among them, PLD is a powerful and flexible technique for fabricating simple and complex metal oxide films, and has several advantages for thin film deposition: (1). Direct stoichiometry transfer from the target to the growing film. (2). High deposition rate and inherent simplicity for the growth of multilayered structures. (3). Dense, textured films can be produced more easily by PLD with in situ substrate heating.

In this work, LiCoO_2 thin films were prepared on the SiO_2/Si substrates by PLD. The microstructure and surface morphology of thin films were characterized by X-ray diffraction (XRD) and Field emission scanning electron microscopy (FESEM). The crack-free and well-crystallized LiCoO_2 thin films with smooth surfaces were used to study the electrochemical behavior and Li diffusion of this material.

II. EXPERIMENTAL

A. Thin film deposition

LiCoO_2 thin films were grown on the Si substrates at a substrate temperature of 600C in an oxygen atmosphere of 100 mTorr for 40 min by PLD with a non-stoichiometric LiCoO_2 target with 15% excess Li_2O to compensate for lithium loss during the deposition. The target-substrate distance was kept at 40 mm. During deposition, the target was rotated at 10-20 rpm to avoid depletion of material at

any given spot. A Lambda Physik KrF excimer laser with wavelength 248 nm was used in the deposition. Laser fluence was controlled at 2Jcm^{-2} and a repetition rate at 10 Hz. In case of the SOS substrate, a double layer of Pt/Ti was deposited on it, where Pt was used as current collector and Ti was used as a buffer layer to enhance the adhesion between the Pt and SiO_2 interface.

B. Microstructure and surface morphology characterization

Structure and crystallinity of the thin film samples were measured using a Shimadzu XRD-6000 X-ray diffractometer with $\text{Cu K}\alpha$ radiation. Data were collected in the 2θ range of $10 - 70^\circ$ at a scan rate of $2^\circ/\text{min}$. Surface morphology and roughness of thin films were characterized using a Hitachi S-4100 Field emission scanning electron microscopy (FESEM). The cross-section of thin film on the SOS substrate was observed by FESEM to estimate the thin film thickness and the growth rate.

C. Electrochemical Measurements

The Li/LiCoO_2 cell was assembled using the LiCoO_2 thin film as the cathode and a lithium metal foil as the anode and a 1 M LiPF_6 in ethyl carbonate/dimethyl carbonate solution (EC/DEC, 1/1 Vol% Ozark Florine Specialties, Inc.) as the electrolyte. All electrochemical experiments were conducted in an Ar-filled glove box using a Solatron 1287 two-terminal cell test system. Galvanostatic charge/discharge tests were carried out between 3 and 4.7 V using a constant current density of $15 \mu\text{A}/\text{cm}^2$. To measure the chemical diffusion coefficient of Li in the Li_xCoO_2 film by potentiostatic intermittent titration technique (PITT), a potential step of 10 mV was applied and the current was measured as a function of time. The potential step was stepped to the next level when the current dropped below $0.1 \mu\text{A}/\text{cm}^2$. This procedure was repeated between 3.88 and 4.50 V at both increasing and decreasing potentials.

III. RESULTS AND DISCUSSION

The layered form of LiCoO_2 , which has rhombohedral symmetry and belongs to the space group $R\bar{3}m$, is ideally suited to accommodate large changes in Li concentration. This crystal structure of closed-packed oxygen layers stacked in an ABC sequence with Co and Li ions residing in octahedral sites in alternating layers between the oxygen planes. Figure 1 illustrates the crystal structure of the layered form of LiCoO_2 . Figure 2 shows the XRD spectra of the bare SOS substrate by itself and of the LiCoO_2 thin film deposited on the substrate. The spectrum of the LiCoO_2 film shows a very strong (003) diffraction peak at 18.90° . Besides the sharp and strong (003) peak, another two small peaks at 38.40° and 59.14° can be attributed to (006) and (009) diffractions of rhombohedral LiCoO_2 . The strong and sharp (003) diffraction peak indicates that the film has a high

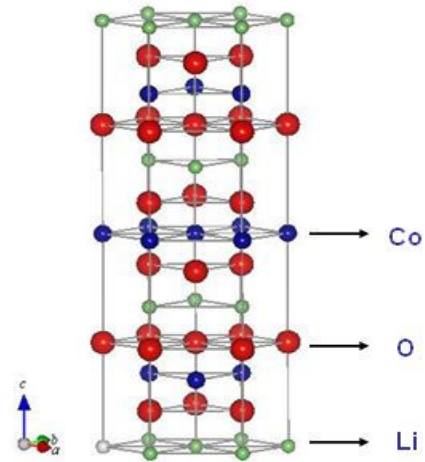


Fig. 1. The crystal structure of the layered form of LiCoO_2 . The oxygen ions form close-packed planes stacked in an ABCABC sequence, and the cobalt and lithium ions occupy alternating layers of octahedral sites.

degree of crystallinity. Other diffraction peaks of LiCoO_2 such as (101) and (104) in this scan range can not be detected, indicating that the film has a preferred c -axis (003) out-of-plane orientation. According to the literature [3,8], all LiCoO_2 thin films will develop the preferred (003) texture no matter what deposition method used when the film is less than $0.5 \mu\text{m}$ thick. The preferred (003) texture of the thin film is due to the lowest surface energy of (003) plane. However, when the film is getting thick ($> 0.5 \mu\text{m}$), the preferred (003) texture will gradually disappear and be replaced by the preferred (101)-(104) texture as a result of the tendency to minimize the volume strain energy developed in the film during the deposition. The preferred (003) texture of the LiCoO_2 film will block the Li diffusion because no Li layer channel is open at the surface to the electrolyte. In this case, Li ion transport is carried mainly through the grain boundaries of the film.

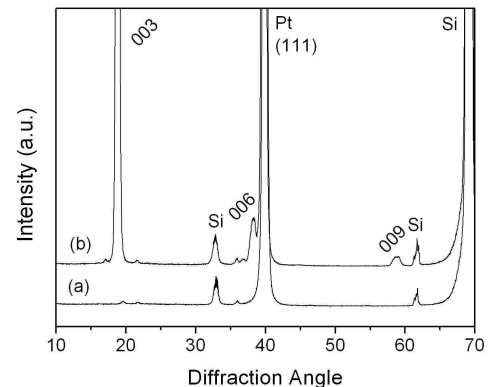


Fig. 2. XRD spectra of: (a) a bare SOS substrate and (b) a LiCoO_2 thin film deposited on the SOS substrate.

Figure 3 shows the FESEM micrographs of the top view and the cross-section view of LiCoO_2 thin films on the SOS

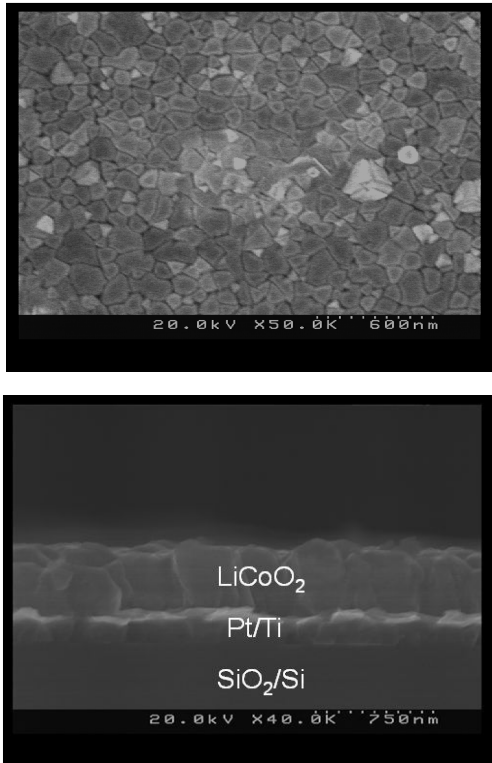


Fig. 3. FESEM micrographs of (a) top view of LiCoO_2 thin film on the SOS substrate and (b) cross-section view of LiCoO_2 thin film on the SOS substrate.

substrates. It can be seen that the film is composed of well-defined grains and has a very smooth surface without any pinholes or cracks. The average grain size is about 200 nm. From the cross-section view of the film on the SOS substrate, we can estimate the thin film thickness is about 300 nm and growth rate of LiCoO_2 thin film by PLD is about 7.5 nm/min.

From the XRD and FESEM results, it is clear that the film deposited by PLD has a high degree of crystallinity with layered structure and well-defined geometry. To further understand the electrochemical behavior of this thin film electrode, charge/discharge measurement was performed between 3 and 4.7 V at a current of $15 \mu\text{A}/\text{cm}^2$ ($C/2$ rate). The typical charge/discharge curves of the LiCoO_2 thin film are shown in Figure 4. It can be seen that the charge and discharge curves are highly reversible with only a small amount irreversible capacity. Though the upper cutoff voltage is as high as 4.7 V, the charge and discharge curve only show a small polarization. According to literature [9,10], the upper cutoff voltage of LiCoO_2 is often limited to 4.2 V, corresponding to extracting and inserting 0.5 Li per LiCoO_2 . Using a higher upper cutoff voltage above 4.2 V often results in fast capacity fade. According to literature [11,12], when LiCoO_2 is slow charged to 4.7 V, almost all lithium ions can be removed from LiCoO_2 . As shown in Figure 4, the charge capacity is about $27 \mu\text{Ah}/\text{cm}^2$ when charged to 4.7 V while the charge capacity is about 15

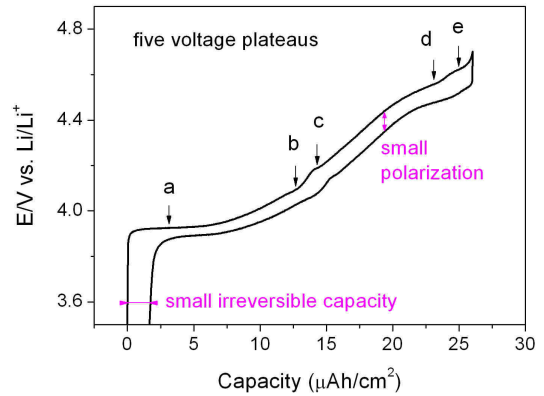


Fig. 4. Typical charge/discharge curves of the Li/LiCoO_2 cell with thin film LiCoO_2 cathode between 3 and 4.7 V at a current of $15 \mu\text{A}/\text{cm}^2$.

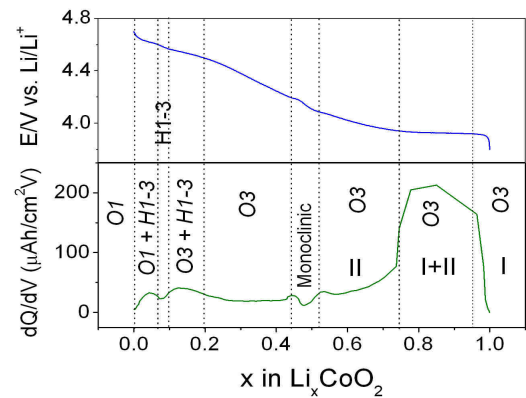


Fig. 5. Voltage profile and the differential capacity, dQ/dV , curve as a function of Li concentration.

$\mu\text{Ah}/\text{cm}^2$ when charged to 4.2 V, which indicates that the film is not really fully delithiated when charged to 4.7 V. This is probably due to the rate limitation at high voltage which limits all lithium ions to be extracted at a fast charge rate. Structural phase transitions are often detrimental to the structural stability of the electrode material and will result in structure degradation and fast capacity fade. As shown in Figure 4, it is clear to see 5 voltage plateaus for both charge and discharge curves. The three voltage plateaus below 4.2 volt are well known in previous studies to LiCoO_2 . The two voltage plateaus above 4.5 V have been found recently from the composite electrode [11] and attributed to two new phase transitions at high voltages.

In order to better understand the phase transitions at different charge states, the voltage profile as a function of Li concentration and the corresponding differential capacity, dQ/dV curves are shown in Figure 5. It is clear to see all phase transitions in all Li concentration range. The phase transition between $0.75 < x < 0.95$ corresponds to the first order metal-insulator transition between two hexagonal phases [13]. Another two phase transitions around $x = 0.5$ correspond to the order/disorder transitions near composition $\text{Li}_{0.5}\text{CoO}_2$ [14]. The observation of another two

phase transitions below $x < 0.2$ agrees well with Chen and Dahn's observation [11] on a LiCoO_2 composite electrode, who attributed these two peaks to the phase transitions from the O3 phase to the H1-3 phase and from the H1-3 phase to the O1 phase, as predicted by Van der Ven and Ceder [15]. The O3 and O1 phase are respectively the rhombohedral and hexagonal form of Li_xCoO_2 , and the H1-3 phase is the stage II compound of Li_xCoO_2 which can be considered as a hybrid of the rhombohedral and hexagonal host. According to Amatuucci et al's paper [16], these two phase transitions accompany severe structure changes, which is probably the reason why fast capacity fade was often observed when LiCoO_2 cycled to 4.7 V.

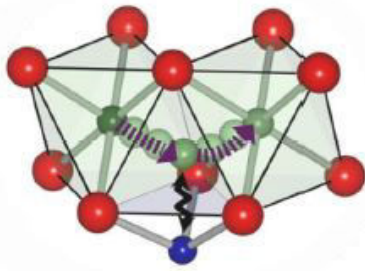


Fig. 6. The diffusion path of Li ion in the layered structure. Li migrates from one octahedral site to another by passing through an intermediate tetrahedral site.

Besides the structural phase transitions at high voltage, Li diffusion is also very important to the performance of LiCoO_2 at high voltages. The Li diffusion mechanism is believed to be the tetrahedral site hop (TSH) mechanism [17]. It is known that Li is coordinated octahedrally by oxygens. If the lithium ion hops into a vacancy that is part of a divacancy then the minimum energy path passes through the tetrahedral site centered between the two vacancies and the initial site of the hop. The schematic diffusion path of lithium ion is shown in Figure 6. As shown in Figure 6, the Li ion migrates from one octahedral site to another by passing through an intermediated tetrahedral site. The tetrahedral site along the TSH migration path shares a face with an oxygen octahedron around a cobalt ion. The lithium ion in the tetrahedral site therefore experiences a large electrostatic repulsion from the positively charged Co ion. The chemical diffusion coefficient of Li in Li_xCoO_2 is expected to be influenced by several factors: (i) the concentration of vacancy sites available for lithium ions to hop, (ii) the activation barrier for lithium ions to hop, and (iii) the thermodynamic factor. The concentration of vacancy sites increases with decreasing Li concentration. As discussed by Van der Ven and Ceder [18], the variation of the activation barrier can be attributed to two factors. One is the c -lattice parameter. A drop of the c -lattice parameter will reduce the distance between the oxygen planes, and compress the tetrahedral site resulting in an increase in the activation barrier. A second factor is the change in effective valence of

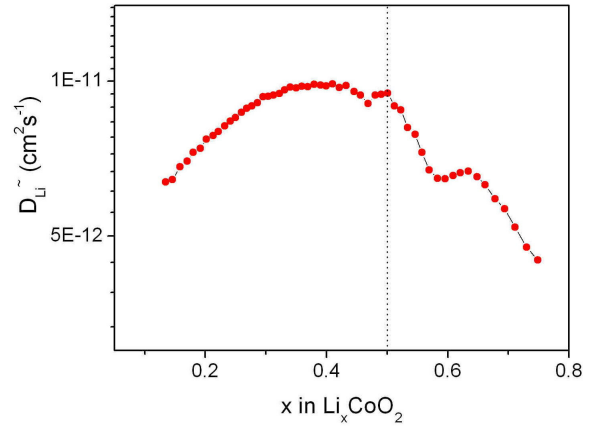


Fig. 7. Chemical diffusion coefficient of Li vs. x in Li_xCoO_2 during charge states by PITT

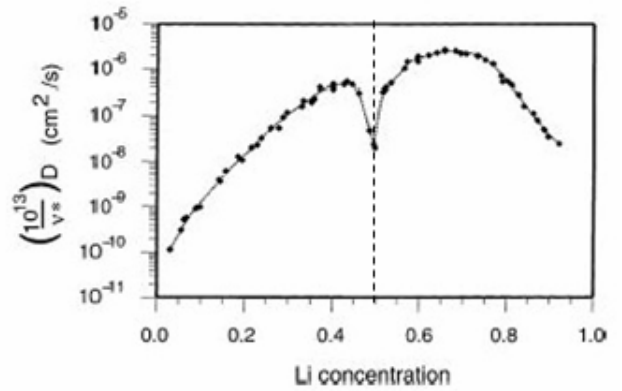


Fig. 8. Calculated value for the chemical diffusion coefficient of Li in Li_xCoO_2 at 400K. (By Van der Ven and Ceder [18])

the cobalt ions with Li concentration. As Li concentration is reduced, the effective positive charge on Co increases causing the activation barrier to increase. The thermodynamic factor is a measure of the deviation of the chemical potential from that for an ideal solution.

Figure 7 shows the chemical diffusion coefficients of Li vs. x in Li_xCoO_2 film during the charge process by PITT. The values of \tilde{D}_{Li} in the Li concentration range $0.15 < x < 0.75$ vary from 10^{-12} to $10^{-11} \text{ cm}^2\text{s}^{-1}$, agreeing well the values obtained previously from LiCoO_2 electrodes [19-20]. Figure 8 shows the calculated value for the chemical diffusion coefficient of Li in Li_xCoO_2 at 400 K by Van der Ven and Ceder [18]. Since a rigorous first-principles calculation of the hop prefactor ν^* , they have normalized the diffusion coefficient in Fig. 8 by $10^{13}/\nu^*$, where 10^{13} sec^{-1} is typically a good approximation for ν^* . It can be seen that our experimental result agree well with the calculated result. In high Li concentration range ($0.5 < x < 0.75$), \tilde{D}_{Li} will increase as the x decreases. In this Li concentration range, the c -lattice parameter increases only slightly with decreasing Li concentration and the activation barrier does not change much. Therefore, in this composition range, the chemical diffusion coefficient of Li is mainly influenced by

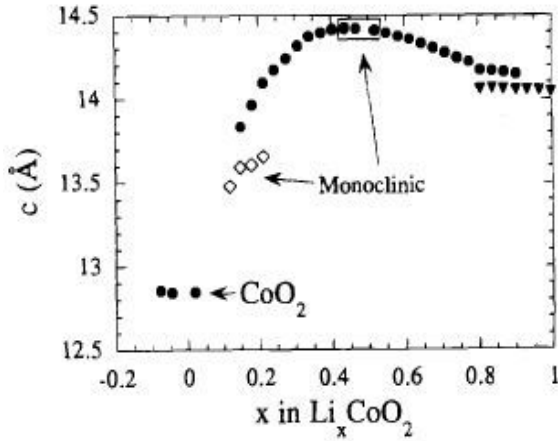


Fig. 9. Variation of c -lattice parameter during lithium extraction of LiCoO_2 . (by Amatuucci et al. [16])

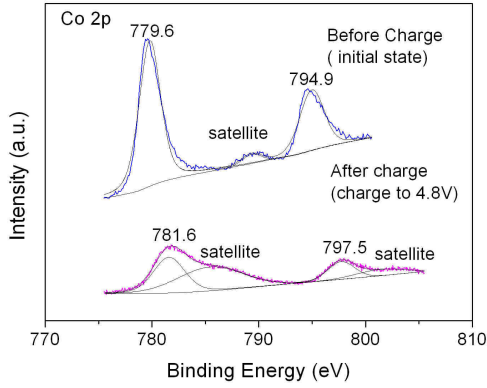


Fig. 10. Co 2p XPS spectra of the as-deposited LiCoO_2 film and film charged to 4.8 V at the surface region.

the increasing concentration of Li vacancies. In low Li concentration range ($x < 0.4$), \tilde{D}_{Li} will decrease as the x decreases. Figure 9 shows the variation of c -lattice parameter during lithium extraction of LiCoO_2 by Amatuucci et al. It is clear that the c -lattice parameter starts to decrease when $x < 0.4$. Therefore when $x < 0.4$, the c -lattice parameter decreases, and the charge on Co ion increases with decreasing Li concentration, resulting in a significant increase in the activation barrier energy.

Though there is a good agreement between the experimental result and previously calculated result for Li diffusivity in LiCoO_2 , an obvious discrepancy exists. As shown in Figure 7, the experimental result shows a maximum at about $x = 0.5$. However, the calculated result shows a minimum at about $x = 0.5$ as shown in Figure 8. The chemical diffusion coefficient \tilde{D}_{Li} is a product of the self-diffusion coefficient D_{Li} and the thermodynamic factor θ . is proportional to $-dV/dx$, which will have minima at the phase boundaries near the composition $\text{Li}_{0.5}\text{CoO}_2$ and a maximum at the composition $\text{Li}_{0.5}\text{CoO}_2$ [21,22]. As discussed by Van der Ven and Ceder [18], the self-diffusion coefficient D_{Li} , should have a minimum at $x = 0.5$ due to the

higher activation energy associated with Li hops in ordered $\text{Li}_{0.5}\text{CoO}_2$. Whether the chemical diffusion coefficient, \tilde{D}_{Li} , is maximal or minimal depends on the balance between the thermodynamic factor and the self-diffusion coefficient. A less-ordered $\text{Li}_{0.5}\text{CoO}_2$ cathode will exhibit a less deep minimum of D_{Li} as there would be less limitation to Li hopping. The thermodynamic factor, on the other hand, is an averaged quantity and is likely to be less drastically influenced by the state of order. Hence in real sample, which are less ordered than in simulations, the thermodynamic factor may dominate and lead to a maximum.

Though it is difficult to measure the chemical diffusion coefficient of Li above 4.5 V ($x < 0.15$) because PITT is only meaningful in a single phase region, it is reasonable to believe that an even faster drop of the Li diffusion will occur when the LiCoO_2 film is further charged to 4.6 and 4.7 V. According to the experimental result by Amatuucci et al. [16] (Figure 9), the c -lattice drops more significantly when LiCoO_2 goes through the two phase transitions from the O3 to the H1-3 phase and from the H1-3 phase to the O1 phase. As discussed previously, a drop of the c -lattice parameter will increase the activation barrier for Li hopping. In the meanwhile, the effective valence of Co ions will increase as the Li concentration decrease, which will also cause the activation barrier to increase. Figure 10 shows the Co 2p XPS spectra of the as-deposited LiCoO_2 film and the film charged to 4.8 V at the surface region. It is clear to see the transformation from Co^{3+} to Co^{4+} during the delithiation. The severe drop of c -lattice parameter and the increase of the effective valence of Co ions above 4.5 V will result in a fast drop of Li diffusion in the material. The structural phase transitions above 4.5 V together with the decreasing Li diffusivity, which makes Li composition gradients larger, likely leads to large internal strains, and subsequent mechanical degradation of the material. Therefore, the sluggish Li diffusion accompanying the large internal strains above 4.5 V for LiCoO_2 may limit the use of LiCoO_2 electrodes at high voltages above 4.5 V.

IV. CONCLUSIONS

Well-crystallized LiCoO_2 thin film electrodes with smooth surfaces have been prepared by PLD on the SOS substrates. The charge/discharge curves of the Li/ LiCoO_2 cell show 5 voltage plateaus between 3 and 4.7 V. Two phase transitions were observed above 4.5 V, which are attributed to the phase transition from the O3 to the H1-3 and the phase transition from the H1-3 to the O1 phase. The chemical diffusion coefficient measured by PITT varies from 10^{-11} to 10^{-12} cm^2/s in the Li concentration range $0.15 < x < 0.75$. The experimental result of Li diffusivity agrees well the calculated result. In high Li concentration range ($x > 0.5$), Li diffusivity increases as the Li concentration decreases due to the increase of the concentration of Li vacancies. In low Li concentration range ($x < 0.4$), Li diffusivity decreases as the

Li concentration decreases due to the drop of the c -lattice parameter and the increase of effective valence of Co ions. The structural phase transitions and the sluggish Li diffusivity above 4.5 V will limit the use of LiCoO₂ electrodes at high voltages above 4.5 V.

ACKNOWLEDGMENT

This research was supported by Advanced Materials for Micro- and Nano- System (AMM&NS) program under Singapore-MIT Alliance (SMA) and by National University of Singapore.

REFERENCES

- [1] K. Mizushima, P. C. Jones, P. J. Wiseman, and J. B. Goodenough, "Li_xCoO₂ (0<x<1): A new cathode material for batteries of high energy density" *Mater. Res. Bull.*, vol. 15, pp. 783–789, June 1980.
- [2] T. Ohzuku, and A. Ueda, "Why transition metal (di) oxides are the most attractive materials for batteries", *Solid State Ionics*, Vol. 69, pp. 201–211, August 1994.
- [3] J. B. Bates, N. J. Dudney, B. J. Neudecker, F. X. Hart, H. P. Jun, and S. A. Hackney, "Preferred orientation of polycrystalline LiCoO₂ films", *J. Electrochem. Soc.*, Vol. 147, pp. 59-70, 2000.
- [4] H. Xia, L. Lu, and G. Ceder, "Substrate effect on the microstructure and electrochemical properties of LiCoO₂ thin films grown by PLD", *J. Alloy & Compd.*, Vol 417, pp. 304-310, 2006.
- [5] S. I. Cho, and S. G. Yoon, "Characterization of LiCoO₂ thin film cathodes deposited by liquid-delivery metalloorganic chemical vapor deposition for rechargeable lithium batteries", *J. Electrochem. Soc.*, Vol. 149, pp. A1584-A1588, 2002.
- [6] J. P. Maranchi, A. F. Hepp, and P. N. Kumta, "LiCoO₂ and SnO₂ thin film electrodes for lithium-ion battery applications", *Mater. Sci & Eng. B.*, Vol. 116, pp. 327-340, 2005.
- [7] W. S. Yoon, S. H. Ban, K. K. Lee, K. B. Kim, M. G. Kim, and J. M. Lee, "Electrochemical characterization of layered LiCoO₂ films prepared by electrostatic spray deposition", *J. Power Sources*, Vol. 97-98, pp. 282-286, 2001.
- [8] Y. Iriyama, M. Inaba, T. Abe, and Z. Ogumi, "Preparation of c -axis oriented thin films of LiCoO₂ by pulsed laser deposition and their electrochemical properties", *J. Power Sources*, Vol.94, pp. 175-182, 2001.
- [9] H. Wang, Y. I. Jang, B. Huang, D. R. Sadoway, and Y. M. Chiang, "TEM study of electrochemical cycling-induced damage and disorder in LiCoO₂ cathodes for rechargeable lithium batteries", *J. Electrochem. Soc.*, Vol.146, pp. 470-472, 1999.
- [10] J. Cho, Y. J. Kim, and B. Park, "Novel LiCoO₂ cathode material with Al₂O₃ coating for a Li ion cell", *Chem. Mater.*, Vol.12, pp. 3788-3791, 2000.
- [11] Z. H. Chen, Z. H. Lu, and J. R. Dahn, "Staging phase transitions in Li_xCoO₂", *J. Electrochem. Soc.*, Vol. 149, pp. A1604-A1609, 2002.
- [12] Y. I. Jang, N. J. Dudney, D. A. Blom, and L. F. Allard, "Electrochemical and electron microscopic characterization of thin-film LiCoO₂ cathodes under high-voltage cycling conditions", *J. Power Sources*, Vol. 119-121, pp. 295-299, 2003.
- [13] C. A. Marianetti, G. Kotliar, and G. Ceder, "A first order Mott transition in Li_xCoO₂", *Nature Materials*, Vol. 3, pp.627-631, 2004.
- [14] J. N. Reimers, and J. R. Dahn, "Electrochemical and in situ X-ray diffraction studies of lithium intercalation in Li_xCoO₂", *J. Electrochem. Soc.*, Vol. 139, pp. 2091-2097, 1992.
- [15] A. Van der Ven, and G. Ceder, "First-principles evidence for stage ordering in Li_xCoO₂", *J. Electrochem. Soc.*, Vol 145, pp.2149-2155, 1998.
- [16] G. G. Amatucci, J. M. Tarascon, and L. C. Klein, "CoO₂, the end member of the Li_xCoO₂ solid solution", *J. Electrochem. Soc.*, Vol.143, pp. 1114-1123, 1996.
- [17] A. Van der Ven, and G. Ceder, "Lithium diffusion in layered Li_xCoO₂", *Electrochem. Solid-State Lett.*, Vol. 3, pp. 301-304, 2000.
- [18] A. Van der Ven, and G. Ceder, "Lithium diffusion mechanisms in layered intercalation compounds", *J. Power Sources*, Vol. 97-98, pp. 529-531, 2001.
- [19] M. D. Levi, G. Salitra, B. Markovsky, H. Teller, D. Aurbach, U. Heider, and L. Heider, "Solid-state electrochemical kinetics of li-ion intercalation into Li_{1-x}CoO₂: simulation application of electroanalytical techniques SSCV, PITT, and EIS", *J. Electrochem. Soc.*, Vol. 146, pp. 1279-1289, 1999.
- [20] Y. I. Jang, B. J. Neudecker, and N. J. Dudney, "Lithium diffusion in Li_xCoO₂ (0.45 < x < 0.7) intercalation cathodes", *Electrochem. Solid-State Lett.*, Vol. 4, pp. A74-A77, 2001.
- [21] H. Xia, L. Lu, and G. Ceder, "Li diffusion in LiCoO₂ thin films prepared by pulsed laser deposition", *J. Power Sources*, Vol. 159, pp. 1422-1427, 2006.
- [22] H. Xia, L. Lu, Y. S. Meng, and G. Ceder, "Phase transitions and high-voltage electrochemical behavior of LiCoO₂ thin films grown by PLD", *J. Electrochem. Soc.*, accepted.